

Electronic Supplementary Information

Unique 3D $\text{Co}^{\text{II}}/\text{Zn}^{\text{II}}$ -coordination polymers with (3,4,5)-connected self-penetrating topology: Syntheses, topological structures, luminescent and magnetic properties

Wen-Wen Dong,^a Dong-Sheng Li,*^{ab} Jun Zhao,^a Ya-Ping Duan,^a Liang Bai^a
and Jing-Jing Yang^a

^a College of Mechanical & Material Engineering, Research Institute of Materials, China
Three Gorges University, Yichang 443002, P. R. China

^b State Key Laboratory of Coordination Chemistry, Nanjing University, Nanjing 210093,
China

RSC-Advances

* Corresponding authors

E-mail address: lidongsheng1@126.com (D.-S. Li), Tel./Fax: +86-717-6397516;

Materials and General Methods

All the solvents and reagents for syntheses were commercially available and used as received. The infrared spectra ($400\text{-}4000\text{ cm}^{-1}$) were recorded as KBr pellets a FTIR Nexus spectrophotometer. Elemental analyses were performed on a Perkin-Elmer 2400 Series II analyzer. Powder X-ray diffraction (PXRD) patterns were taken on a Rigaku Ultima IV diffractometer (Cu $\text{K}\alpha$ radiation, $\lambda = 1.5406\text{ \AA}$), with a scan speed of $8^\circ/\text{min}$ and a step size of 0.02° in 2θ . The calculated PXRD patterns were simulated by using the single-crystal X-ray diffraction data. Thermogravimetric (TG) curves were recorded on a NETZSCH STA 449C microanalyzer in air atmosphere at a heating rate of $10^\circ\text{C}\cdot\text{min}^{-1}$. the fluorescent property and fluorescence lifetime were recorded on a EDINGBURGH INSTRUMENTS-FLS920. Variable-temperature magnetic susceptibility measurements (2-300 K) were carried out on a Quantum Design PPMS60000 in a magnetic field of 1KOe, and the diamagnetic corrections were evaluated by using Pascal's constants.

Crystallographic data collection and refinement

The data collections were performed at $293(2)\text{K}$ on a Bruker SMART APEX CCD diffractometer using graphite-monochromatic Mo $\text{K}\alpha$ radiation ($\lambda = 0.71073\text{ \AA}$). Absorption corrections were made with the program SADABS [1], and the crystallographic package SHELXTL [2] was used for all calculations. Metal atoms in complex 1 were located from the *E*-maps and other non-hydrogen atoms were located in successive difference Fourier syntheses, which were refined with anisotropic thermal parameters on F^2 . The H atoms of the ligands were generated theoretically onto the specific atoms and refined isotropically with fixed thermal factors. The H atoms of the water molecules were located using the difference Fourier method and constrained refinement. CCDC 847910 and 873469 contain the supplementary crystallographic data for this paper.

References

- [1] G. M. Sheldrick, SADABS, Program for area detector adsorption correction, Institute for Inorganic Chemistry, University of Göttingen, Germany, 1996.
- [2] G. M. Sheldrick, SHELXL-97, Program for refinement of crystal structures, University of Göttingen, Germany, 1997; SHELXTL Reference Manual, Version 5.1, Bruker AXS, Analytical X-Ray Systems, Inc., Madison, WI, USA, 1997.

Table S1. Selected bond lengths (\AA) and bond angles ($^\circ$) for **1** and **2**

1^a					
Co(1)-O(7)#1	1.999(4)	Co(2)-O(2)#4	2.013(4)	Co(3)-O(9)	2.043(4)
Co(1)-N(3)	2.040(5)	Co(2)-O(1)	2.031(4)	Co(3)-O(8)#5	2.047(4)
Co(1)-O(3)#2	2.080(4)	Co(2)-N(7)	2.157(4)	Co(3)-N(11)	2.052(4)
Co(1)-N(1)#3	2.099(5)	Co(2)-O(6)	2.160(4)	Co(3)-N(12)#6	2.082(4)
Co(1)-N(5)	2.226(4)	Co(2)-O(5)	2.180(4)	Co(3)-N(8)	2.187(4)
Co(1)-O(4)#2	2.275(5)	Co(2)-N(6)	2.191(4)		
O(7)#1-Co(1)-N(3)	106.48(2)	N(1)#3-Co(1)-O(4)#2	93.80(2)	O(2)#4-Co(2)-O(1)	116.12(2)
O(7)#1-Co(1)-O(3)#2	101.33(2)	O(5)-Co(2)-N(6)	96.00(2)	O(2)#4-Co(2)-N(7)	91.25(2)
N(3)-Co(1)-O(3)#2	146.02(2)	O(1)-Co(2)-N(7)	91.14(2)	O(6)-Co(2)-N(6)	91.41(2)
O(7)#1-Co(1)-N(1)#3	90.8(2)	O(2)#4-Co(2)-O(6)	90.16(2)	O(9)-Co(3)-N(11)	97.47(2)
N(3)-Co(1)-N(1)#3	102.27(2)	O(1)-Co(2)-O(6)	153.49(2)	O(8)#5-Co(3)-N(11)	158.17(2)
O(3)#2-Co(1)-N(1)#3	96.39(2)	N(7)-Co(2)-O(6)	91.80(2)	O(9)-Co(3)-N(12)#6	100.66(2)
O(7)#1-Co(1)-N(5)	84.59(2)	O(2)#4-Co(2)-O(5)	150.13(2)	O(8)#5-Co(3)-N(12)#6	93.87(2)
N(3)-Co(1)-N(5)	76.90(2)	O(1)-Co(2)-O(5)	93.75(2)	N(11)-Co(3)-N(12)#6	101.92(2)
O(3)#2-Co(1)-N(5)	86.82(2)	N(7)-Co(2)-O(5)	87.90(2)	O(9)-Co(3)-N(8)	86.13(2)
N(1)#3-Co(1)-N(5)	174.86(2)	O(6)-Co(2)-O(5)	60.05(1)	O(8)#5-Co(3)-N(8)	85.94(2)
O(7)#1-Co(1)-O(4)#2	161.18(2)	O(2)#4-Co(2)-N(6)	86.09(2)	N(11)-Co(3)-N(8)	76.59(2)
N(3)-Co(1)-O(4)#2	90.34(2)	O(1)-Co(2)-N(6)	87.17(2)	N(12)#6-Co(3)-N(8)	173.19(2)
O(3)#2-Co(1)-O(4)#2	60.05(2)	N(7)-Co(2)-N(6)	175.85(2)	O(9)-Co(3)-O(8)#5	94.25(2)
N(5)-Co(1)-O(4)#2	91.28(2)				
2^b					
Zn(1)-O(7)#1	2.028(3)	Zn(2)-O(3)#1	2.015(3)	Zn(3)-O(4)#3	2.005(3)
Zn(1)-N(5)	2.303(3)	Zn(2)-O(2)	2.041(3)	Zn(3)-N(10)	2.013(3)
Zn(1)-N(1)#2	2.068(3)	Zn(2)-O(9)#3	2.156(3)	Zn(3)-O(6)	2.016(3)
Zn(1)-N(3)	2.043(3)	Zn(2)-N(6)	2.191(3)	Zn(3)-N(7)#4	2.078(4)
Zn(1)-O(1)	2.048(3)	Zn(2)-N(12)	2.215(3)	Zn(3)-O(5)#3	2.422(4)
O(7)#1-Zn(1)-N(3)	154.65(14)	Zn(2)-O(8)#3	2.232(3)	Zn(3)-N(11)	2.489(4)
N(1)#2-Zn(1)-N(5)	170.24(14)	O(3)#1-Zn(2)-O(2)	118.20(13)	O(4)#3-Zn(3)-N(10)	137.90(14)
O(1)-Zn(1)-N(5)	87.93(13)	O(3)#1-Zn(2)-N(12)	87.75(12)	O(5)#3-Zn(3)-N(11)	90.33(16)
N(3)-Zn(1)-N(5)	74.61(12)	O(9)#3-Zn(2)-N(6)	88.14(13)	N(7)#4-Zn(3)-N(11)	172.48(14)
O(7)#1-Zn(1)-N(5)	83.32(12)	O(2)-Zn(2)-N(6)	89.71(13)	O(6)-Zn(3)-N(11)	80.41(14)
O(1)-Zn(1)-N(1)#2	101.83(13)	O(3)#1-Zn(2)-N(6)	91.96(12)	N(10)-Zn(3)-N(11)	72.95(13)
N(3)-Zn(1)-N(1)#2	103.63(13)	O(2)-Zn(2)-O(9)#3	146.55(12)	O(4)#3-Zn(3)-N(11)	83.03(13)
O(7)#1-Zn(1)-N(1)#2	95.98(12)	N(12)-Zn(2)-O(8)#3	90.71(13)	N(7)#4-Zn(3)-O(5)#3	97.18(16)
N(3)-Zn(1)-O(1)	98.15(14)	N(6)-Zn(2)-O(8)#3	92.20(13)	O(6)-Zn(3)-O(5)#3	163.27(13)

O(7)#1-Zn(1)-O(1)	93.30(13)	O(9)#3-Zn(2)-O(8)3	59.38(11)	N(10)-Zn(3)-O(5)#3	87.61(14)
N(6)-Zn(2)-N(12)	173.90(13)	O(2)-Zn(2)-O(8)#3	87.37(12)	O(4)#3-Zn(3)-O(5)#3	57.93(12)
O(3)#1-Zn(2)-O(9)#3	95.23(12)	O(3)#1-Zn(2)-O(8)3	154.10(12)	O(6)-Zn(3)-N(7)#4	92.37(15)
O(2)-Zn(2)-N(12)	85.07(13)	O(4)#3-Zn(3)-O(6)	106.77(14)	N(10)-Zn(3)-N(7)#4	106.92(14)
O(9)#3-Zn(2)-N(12)	97.95(13)	N(10)-Zn(3)-O(6)	102.74(15)	O(4)#3-Zn(3)-N(7)#4	101.21(14)

^a Symmetry codes for **1**: #1 -x+1, -y, -z+2; #2 x, y, z+1, z+1/2; #3 x-1/2, -y+1/2; #4 -x+1, -y, -z+1; #5 x, y, z-1; #6 x+1/2, -y-1/2, z-1/2;

^b Symmetry codes for **2**: #1 -x+1, -y+1, -z+1; #2 x+1/2, -y+3/2, z-1/2; #3 -x+1, -y+1, -z+2; #4 x-1/2, -y+1/2, z+1/2.

Table S2 Summary of the linking modes of the 10- and 12-membered shortest ring within 3D net

Cycle 1	Cycle 2	Chain ^a	Cross ^b	Mult ^c
10a	10g	1	1	2
10a	12a	1	1	2
10a	12f	1	1	2
10a	12g	1	1	1
10a	12h	1	1	1
10a	12i	1	1	1
10a	12j	1	1	1
10g	10a	1	1	2
10g	12a	1	1	2
10g	12b	1	1	2
12a	8c	1	2	1
12a	10a	1	1	2
12a	12b	1	1	2
12a	12f	1	1	2
12b	10g	1	1	2
12b	12a	1	1	2
12b	12f	1	1	2
12b	12g	1	1	2
12b	12h	1	1	1
12b	12i	1	1	1
12b	12j	1	1	1
12f	10a	1	1	1
12f	10a	1	2	2
12f	12a	1	1	1
12f	12b	1	1	2
12f	12f	1	2	1
12g	10a	1	1	1
12g	12b	1	1	1

12h	10a	1	1	1
12h	12b	1	1	1
12i	10a	1	1	1
12i	12b	1	1	1
12j	10a	1	1	1
12j	12b	1	1	1

^a Chain: the bond amount of the shortest chain that interconnected two rings.

^b Cross: the times of each ring crossing another ring.

^c Mult: the ring numbers of each ring crossed by other on

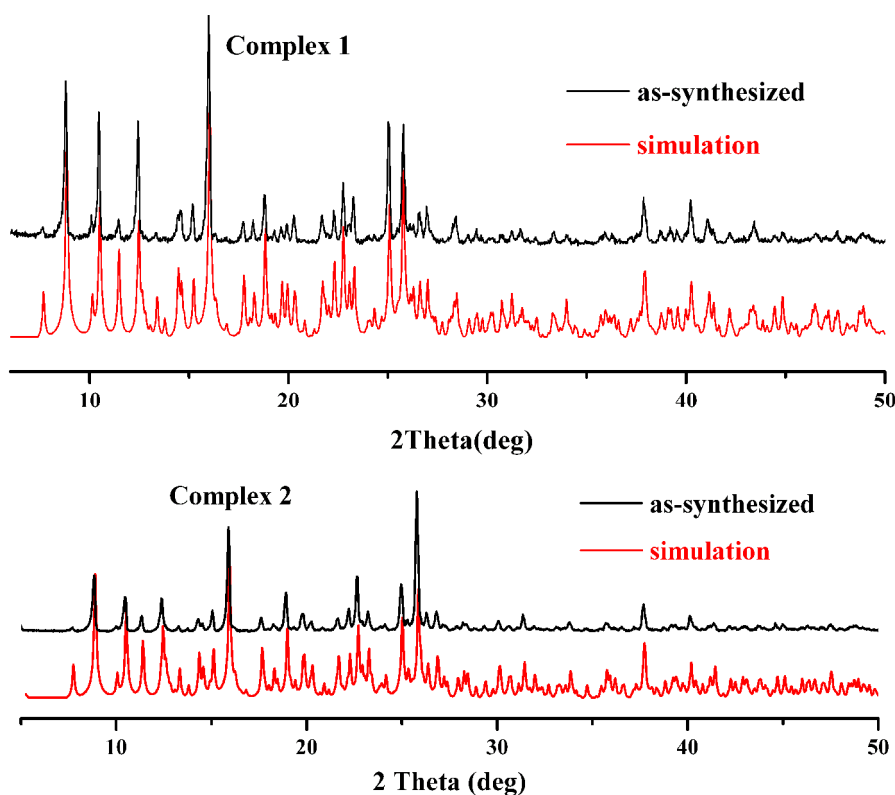


Fig. S1. The PXRD patterns of **1** and **2**. (the red curve for the simulated from the single-crystal, the black curve for experimental data)

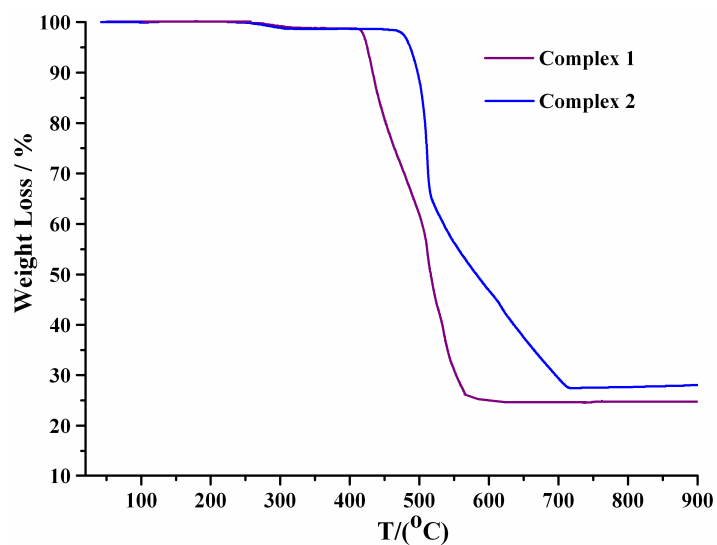


Fig. S2 TGA curves of complexes **1** and **2**.

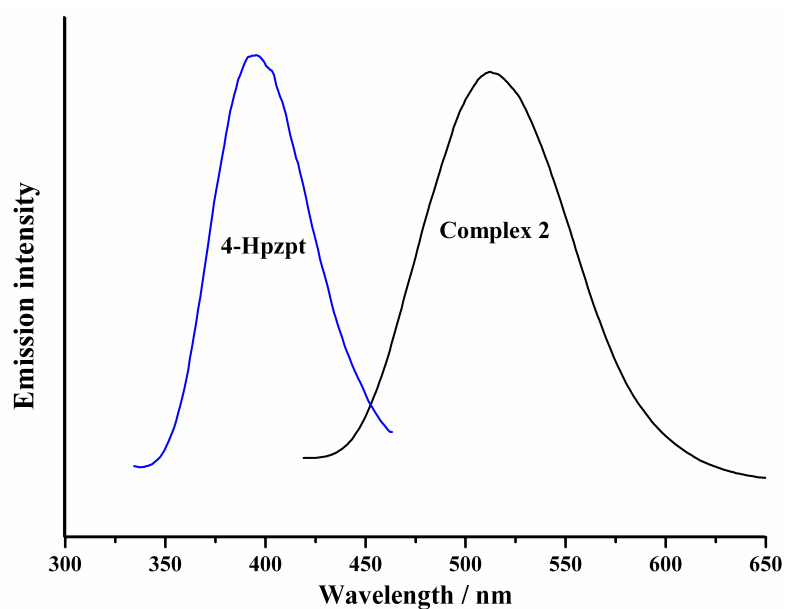


Fig. S3 Solid-state fluorescence emission recorded at room temperature for compound **2** (black) and 4-Hpzpt (blue).

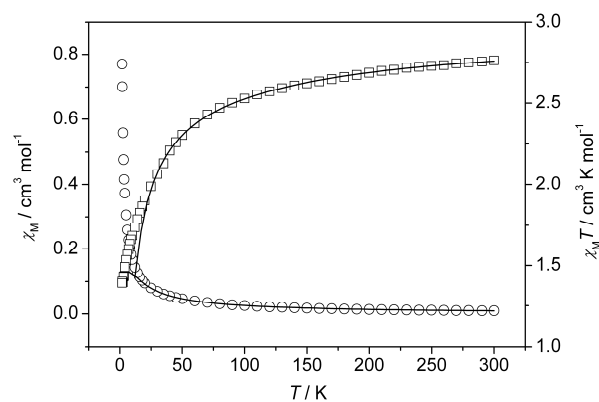


Fig. S4 Plots of $\chi_M T$ vs T (□) and χ_M vs T (○) for **1**. Solid lines represent the fit through simple phenomenological equation
$$\chi_M T = A \exp(-E_1/kT) + B \exp(-E_2/kT)$$

Here, $A + B$ equals the Curie constant, and E_1, E_2 represent the “activation energies” corresponding to the spin-orbit coupling and the antiferromagnetic exchange interaction. This equation adequately describes the spin-orbit coupling, which results in a splitting between discrete levels, and the exponential low-temperature divergence of the susceptibility [$\chi_M T \propto \exp(\alpha J/2kT)$]. Moreover, it is in excellent agreement with the experimental data obtained in the present work (Figure 4). The obtained values of $A + B = 2.93 \text{ cm}^3 \text{ K mol}^{-1}$ and $E_1/k = 151 \text{ K}$ (using a least-squares fitting method) are consistent with those given in the literature for the Curie constant and for the effect of spin-orbit coupling and site distortion. As for the value found for the antiferromagnetic exchange interaction, it is very weak indeed ($-E_2/k = -0.28 \text{ K}$), corresponding to $J = -0.56 \text{ K}$ according to the Ising chain approximation [see above; $\chi T \sim \exp(+J/2kT)$].